https://doi.org/10.1016/j.resconrec.2019.02.036

Industrial Wastewater Desalination under Uncertainty in Coal-Chemical Eco-Industrial Parks

Liu Huang[a], Dongliang Wang[b], Chang He[c]*, Ming Pan[c], Bingjian Zhang[c], Qinglin Chen[c], Jingzheng Ren[d]

[a] School of Chemistry and Chemical Engineering, Guangdong Pharmaceutical University, Zhongshan 528458, China

[b] School of Petrochemical Engineering, LanZhou University of Technology, LanZhou 730050, China

[c] School of Chemical Engineering and Technology, Guangdong Engineering Technology Research Center for Petrochemical Energy Conservation, Sun Yat-Sen University, Guangzhou 510275, China

[d] Department of Industrial and Systems Engineering, The Hong Kong Polytechnic University, Hong Kong, China

* Corresponding author:

E-mail address: hechang6@mail.sysu.edu.cn (Chang He)

Abstracts:

This work proposes a stochastic multi-scenario model for the robust design of industrial wastewater desalination under uncertainty. For fully accommodating the diverse nature of wastewater variability, multiple uncertain design parameters consisting of salt concentration, flowrate, and inlet temperature of wastewater are taken into account for the realization of uncertainty. A three-step stochastic strategy for data processing including uncertainty characterization and quantification, data sampling, and data propagation is developed to generate a proper size of feeding scenarios. The detailed process model of the dual-stage reverse osmosis is incorporated in the optimization model for minimizing the expected specific production cost. Finally, we illustrate the applicability and effectiveness of the proposed stochastic multi-scenario model with an example from a coal-chemical eco-industrial park.

Keywords: wastewater desalination; uncertainty; reverse osmosis; data processing strategy; robust design

1. Introduction

Coal is recognized as a primal energy source in many developing countries like China that is widely used for producing synthetic chemicals and fuels due to its low acquisition cost and huge geological reserves. However, this development activity has drawn serious attention for a long time for its heavy environmental footprints that can be largely due to wastewater-related issues with the shrinking supplies of freshwater. (Zhu et al., 2017) Compared to other process industries such as refinery, the coal-chemical industry is more dependent on freshwater and normally generates a larger amount of wastewater with complex impurities which bring about particularly intense concerns on sustainability. In response to such concerns, the majority of countries and regions have sanctioned forceful regulations in order to push corporations and seek more efficient and sustainable strategies. (Andiappan et al., 2016; Da et al., 2017) For example, coal-chemical eco-industrial parks (EIPs) have been designed to encourage interplant water and mass exchange for minimizing the freshwater consumption and wastewater generation. (Tiu and Cruz, 2017)

In coal-chemical EIPs, in general there are various co-located industrial facilities such as pre-treatment, gasification, air separation, sweetening, power plant, chemical synthesis, utilities, etc. In these facilities, quantities of freshwater are consumed for washing, separating, heating, reacting, and other basic operations, which in turn result in various waste effluents containing different types of impurities including inorganic, organic, and biological ones in a separate or joint form.(Gupta et al., 2012; Gençer and Agrawal, 2018) Up to 99% of these impurities are required to remove by

combined unit operations and processes, namely primary, secondary, and tertiary water treatments (Yang et al., 2014) and then the wastewater is converted into desired quality water that can be used for multiple types of purpose, e.g., circulating, drinking, demineralized, process supplies. Among these impurities, note that the total dissolved salts (TDS, e.g., Cl^-, SO_4^{2-}, Na^+, Mg^{2+}, and Ca^{2+}) in wastewater have increasingly become a focus of attention for coal-chemical facilities, because they are easy to accumulate in each basic operation but extremely hard to be disposed of. Traditionally, the saline wastewater was diluted and discharged into the environment due to lack of technical and economic feasibilities. Nevertheless, this approach not only fails to reduce the pollutant emissions and freshwater consumption, but also causes the mineralization of freshwater and the alkalinity of soil. It should be mentioned that currently process industries have more stringent treatment standards in practice. For example, a number of coal-chemical EIPs have required the enterprises to operate with zero liquid discharge due to the concerns over waste disposal of the high-concentration brine. (Werber et al., 2017)

Multiple desalination methods can be applied for the treatment of industrial saline wastewater with high TDS concentration, which includes membrane and thermal-based technologies. Recently, membrane-based, pressure-driven reverse osmosis (RO) which selectively allows the passage of water across the membrane modules becomes an attractive desalination solution. It makes up the majority of new installations largely due to its low operating costs and high separation efficiency (Wang et al., 2014). Note that, industrial saline wastewater desalination should be

operated in high water recoveries (i.e., >90%) as efficiently as possible to remove almost all of the dissolved solids from water. Achieving a such high recovery is technologically challenging in practice largely owing to the augment of concentration factor (the concentration ratio of brine and feed water), which leads to drastically decreased permeate flux and increased osmotic pressure difference. (Malaeb and Ayoub, 2011; Werber et al., 2017) Thus, although the specific energy consumption (SEC, $kW \cdot m^{-3}$) is relatively lower than that of seawater desalination, saline wastewater desalination still requires substantial energy input as operated at high recoveries. Some authors have directed their efforts to reduce the energy consumption via process integration and optimization. For instance, El-Halwagi (1997) proposed a detailed mathematical model for RO desalination that allows for process modeling and optimization. Abass and Majozi (2016) and Khor et al. (2012) further developed superstructure-based optimization approaches for the synthesis of a RO-based multi-regenerator network for minimizing water and energy consumption.

In coal-chemical EIPs, the saline wastewaters generated by different plants are normally considered to mix and treat in a centralized treatment facility using a multi-stage desalination process. Note that the saline wastewater streams in different seasons are considerably more variable in solution concentration, flowrate and inlet temperature. In recent years, design, modeling and optimization of process systems with consideration of uncertainty have garnered increasing attention by the literature. For example, the optimal design of RO processes under various product specification and feed concentration has been investigated by Lu et al. (2007); Park et al. (2010)

developed a new stochastic approach to evaluate the operation and construction cost of a seawater RO desalination plant. Onishi et al. (2017a, 2017b) presented a process optimization scheme for zero-liquid discharge desalination process of shale gas flowback water with consideration of uncertainties on the feed water salinity and flowrate. They proposed a new sampling technique to generate a proper set of correlated feeding scenarios. Diwekar and co-workers (Shastri and Diwekar, 2010; Subramanyan et al., 2011) proposed a standardized four-step approach for uncertainty analysis that includes uncertainty characterization, data sampling, propagation and analysis of results. In spite of these efforts, special study on industrial saline wastewaters desalination under uncertainty is hardly found in literature and there is a need to develop systematic strategies to obtain a more precise and robust solution.

This work presents a stochastic multi-scenario model for the robust design of a dual-stage industrial wastewater reverse osmosis (IWRO) desalination process while explicitly accounting for the wastewater variability. The detailed model of the IWRO is included in the objective function in order to give a true cost representation in terms of specific production cost denoting desalination cost per m^3 of permeate product. In this multi-scenario model, solution concentration, flowrate, and inlet temperature of feed wastewater are treated as uncertain design parameters and are taken into account for the realization of uncertainty. A three-step stochastic strategy for data processing including uncertainty characterization and quantification, data sampling, and data propagation is developed to generate a proper size of correlated feeding scenarios to fully accommodate the diverse nature of wastewater variability. An illustrative

example from a coal-chemical EIP is used to evaluate the applicability of the proposed model.

2. Problem definition

The problem addressed in this work can be stated as follows: Given is a stream of saline wastewater generated from a coal-chemical EIP, which are considered as process sources to be regenerated using an IWRO treatment process. In this process, the design problem is considered to have two RO blocks to reach the final permeate product specification with salinity less than 500 ppm. Note that the first and second RO stages employed are designed for brackish water and seawater demineralization, respectively. Each RO stage has known capital cost, membrane properties, allowable water recovery ratio and applied pressure, permeate and brine quality specifications. In addition, the other process equipment (i.e., pumps and energy recovery device) have known lifespan, annual running time, capital costs, allowable operating pressures, efficiencies, utility prices, and possible connections.

In the stochastic problem, the flow rate, salinity, and temperature of the wastewater are regarded as uncertain parameters of the IWRO desalination system. It is assumed that these parameters have known multivariate normal distributions, which can be explicitly expressed through a finite size of correlated feeding scenarios with given probability of occurrence. This stochastic multi-scenario model is optimized to obtain robust solutions through minimizing the mean value of production costs of permeate product for the system. This objective function accounts for the capital investment in the all equipment, as well as the operational expenses related to the

membrane clean and replacement, chemicals, and external utilities, etc., used in the system. The stochastic approach can also determine the optimal numbers of membrane elements and pressure vessels for all scenarios, as well as the energy consumption of permeate, applied pressures of each stage RO, pump sizes, retentate flowrate, splitting ratio, and the preheated temperature of wastewater, etc., for each scenario. To present the advantage of this approach, it is worth noting that this study also introduces a deterministic model where a single set of process variables and particularly the representative data of inlet wastewater including flowrate, salinity, and temperature are considered to minimize the production cost of permeate product.

3. Model Description

In this section, we describe the detailed mathematical model of the dual-stag IWRO desalination process that aims to illustrate how they are optimized using a multi-scenario approach. To reduce the computational burden, we ignore the following items throughout the modelling (a) the temperature change across the membrane channel in the RO module (Wang, et al., 2018); (b) removal of mixture salts like Na_2SO_4 is not considered in the pretreatment process; (c) the influence of feed temperature on the salt passage across the membrane is ignored (Li, 2015); (d) the membrane is isothermal and the temperature of feed wastewater is equal to the dry bulb temperature.

3.1 IWRO treatment model

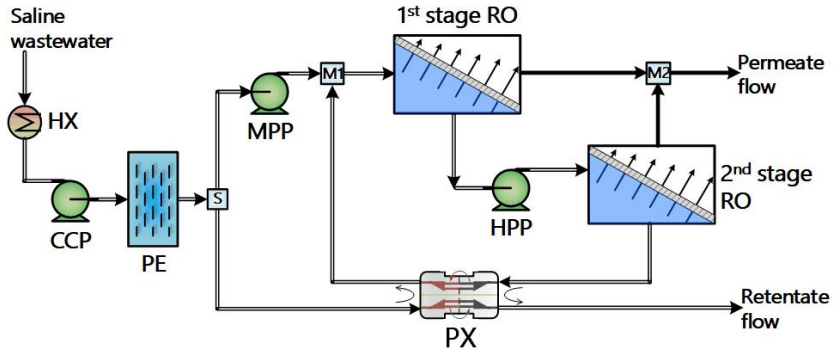

Figure 1. Schematic diagram of the dual-stage IWRO desalination process

To be in line with actual industrial desalination processes, as illustrated in Fig. 1, a once-through, dual-stage RO treatment model with energy recovery device is employed in the present study. As shown, a high-flow, low-pressure intake pump (IP) that pumps the preheated saline wastewater from the heat exchangers (HX) to the suction of the pretreatment unit (PE, e.g., membrane filtration and chemical dose injection (Ghobeity and Mitsos, 2010). The pretreated feed water stream is then split into two branches at point S. The upper branch to the first-stage RO is directly pressurized by mid-pressure feed pump (MPP) to meet a desired feed pressure, while the lower branch is pressurized by pressure exchangers (PX). The retentate of the first-stage RO is introduced to the second-stage RO by a high-pressure feed pump (HPP) for undergoing a deeper desalination. Note that each RO block consists of several pressure vessels in parallel, and each pressure vessel contains a number of interconnected membrane elements. Herein, spiral-wound FILMTEC BW30-400 elements and SW30-400 @ elements (FILMTEC™, 2018) which respectively designed for brackish water and seawater demineralization are employed for the first- and second-stage RO in this study. More details of the properties of these membrane

elements are listed in Table 1. The resulting permeate products with 500 ppm salinity specification leaving these two RO stages are collocated at point M_2. To maximize energy recovery, the retentate stream of second-stage RO with a relatively high pressure exchanges pressure energy using PX with part of the feed stream to raise the pressure that equals to the feed pressure of the first-stage RO. Finally, the depressurized retentate stream with a hyper-salinity of 6.0%~9.0% is introduced to a mechanical vapor recompression unit or evaporation pond for salt crystallization and precipitation.

3.2 Mass and energy balances

Mass balance. According to the solution diffusion model (Wang et al., 2014), the separation performance of RO membranes is mainly determined by the difference between permeate and solute permeabilities. For each stage RO, the permeate flux across a membrane element is proportional to the the net driving pressure P_i^{net} and membrane permeability A_i, as given by

$$J_i^{\mathrm{P}} = A_i\, P_i^{net} = A_i\, (\Delta P_i^{\mathrm{F}} - \overline{\Delta\Pi_i} - \Delta P_i^{d}\,/\,2) \qquad i=1,\,2 \qquad (1)$$

where ΔP_i^{F} is the transmembrane pressure of the feed stream, $\overline{\Delta\Pi_i}$ is the actual osmotic pressure difference, $\Delta P_i^{d}/2$ is the average pressure drop between the retentate and feed streams. The membrane permeability is given by the following equation

$$A_i = A_{ref} \times \mathrm{FF} \times \mathrm{TCF} \qquad (2)$$

where A_{ref} is the water permeability at the reference temperature, FF is the membrane fouling factor, TCF is the temperature correction factor. Herein, note that the higher the temperature of feed stream (T_{F}), the higher the permeate flow rate. The influence

of feed stream temperature on membrane permeability is evaluated by the TCF via an Arrhenius-like correlation:

$$TCF = \begin{cases} \exp[2640 \times (\frac{1}{298} - \frac{1}{T_{\mathrm{F}}})], & T_{\mathrm{F}} > 298K \\ \exp[3020 \times (\frac{1}{298} - \frac{1}{T_{\mathrm{F}}})], & T_{\mathrm{F}} \le 298K \end{cases} \quad (3)$$

For each stage RO, $\overline{\Delta\Pi_i}$ is a function of the feed stream (Π_i^{F}), concentration polarization factor (CPF_i), and the concentration of the feed and retentate streams (C_i^{F} and C_i^{R}), as given by Eq. 4.1. Note that, increasing the recovery ratio per pressure vessel (RR_i) intensifies the phenomenon of concentration polarization. As such, CPF_i that depends on the average recovery ratio can be approximated by Eq. 4.2. (Asatekin et al., 2007) Besides, considering that feed stream contains only NaCl salts, Π_i^F is calculated by the Van't Hoff equation in Eq. 4.3.

$$\overline{\Delta\Pi_i} = CPF_i \times \frac{C_i^R}{C_i^F} \times \Pi_i^F \qquad i = 1,2 \qquad (4.1)$$

$$CPF_i = \exp(\frac{0.7 \times RR_i}{N_i^{pv}}) \qquad i = 1,2 \qquad (4.2)$$

$$\Pi_i^F = \frac{2\rho RT_F}{M_{\mathrm{NaCl}}}(C_i^{\mathrm{R}} - C_i^{\mathrm{F}}) \qquad i = 1,2 \qquad (4.3)$$

where N_i^{pv} is the number of membrane elements inside a pressure vessel; M_{NaCl}, R, and ρ are molar mass of NaCl, universal gases constant, and mass density of the stream, respectively.

The concentration of salts in the permeate and retentate flows can be approximated by the following equations

$$C_i^{\mathrm{P}} = (1 - sr)C_i^{\mathrm{F}} \quad (5)$$

$$C_i^{\mathrm{R}} = \frac{sr \times C_i^{\mathrm{F}}}{1 - RR_i} \tag{6}$$

where *sr* is the membrane's salt rejection factor, which denotes the ratio of salt flux in feed stream not across the membrane element.

The total permeate flow rate of the system is calculated by:

$$Q_P = S^e N^e \sum_{i=1,2} J_i^{\mathrm{P}} \tag{7}$$

where N_i^e and S_i^e are the number of membrane elements inside a RO stage and the active surface area for a membrane element, respectively.

Table 1 Membrane Parameters (Karuppiah et al., 2012; Williams et al., 2012)

Item	***Unit***	***Default***
Active surface of an element, S^e	m^2	37
Number of elements per vessel, N^e	-	7
Element pressure drop, ΔP	bar	0.2
Fouling factor, FF	-	0.85
Water permeability, A_{ref}	10^{-9} kg·m^2·s^{-1}·Pa^{-1}	SW30-400: 3.5 BW30-400: 7.5
Molar mass of NaCl, M_{NaCl}	kg·mol^{-1}	0.0585
Universal gases constant, R	J mol^{-1}·K^{-1}	8.3145
Salt rejection factor, sr	-	0.9975
Temperature of feed stream, T_F	K	see SI

Energy balance. In this process, the work requirement for the low-pressure intake pump is given by the following equations:

$$W_{\mathrm{IP}} = \frac{Q_{\mathrm{F}}}{\eta_{\mathrm{IP}}}(P_1^{\mathrm{F}} - P_{atm}) \tag{8.1}$$

$$Q_{\mathrm{F}} = \frac{Q_{\mathrm{P}}}{\left[RR_1(1-RR_2)+RR_2\right]} \tag{8.2}$$

where Q_{F} is the flow rate of the feed stream, η_{IP} is the overall efficiency of the intake pump, P_{atm} and P_1^{F} are the atmospheric pressure and the feed pressure of the first stage RO, respectively. Considering the pressure loss in pretreatment unit (ΔP_d^{PE}) and minimum inlet pressure at the suction of mid-pressure pump (P_1^{F}), the gaining pressure of the feed stream by intake pump is typically 4~6 bar.

The work required by the mid- and high-pressure feed pumps constitutes the main energy consumption of the IWRO process. The mid-pressure pump is employed to raise the pressure of upper branch of PE outlet from $P_{\mathrm{IP}}-\Delta P_d^{\mathrm{PE}}$ to close to P_1^{F} , thus $\Delta P_{\mathrm{MMP}}= P_1^{\mathrm{F}} -P_{\mathrm{IP}}+ \Delta P_d^{\mathrm{PE}}$. Likewise, the pressure increment by high-pressure pump is $\Delta P_{\mathrm{HHP}}= P_2^{\mathrm{F}} - P_1^{\mathrm{R}}$. The flow rate of the feed stream allocated to the pressure exchangers is dependent on the pressure energy recovered by PX, and the allocating ratio is $Sp=Q_{\mathrm{R}}(P_2^{\mathrm{R}}-P_{out})\,\eta_{\mathrm{PX}}\,\Delta P_{\mathrm{MMP}}$. Thus, the work required to pressurize the feed stream by the mid- and high-pressure feed pumps are computed as:

$$W_{MMP} = [Q_{\mathrm{F}}\Delta P_{\mathrm{MMP}} - Q_{\mathrm{R}}(P_2^{\mathrm{R}}-P_{out})\eta_{\mathrm{PX}}]\frac{1}{\eta_{\mathrm{MMP}}} \tag{8}$$

and

$$W_{\mathrm{HPP}} = Q_{\mathrm{F}}(1-RR_1)\frac{(P_2^{\mathrm{F}}-P_1^{\mathrm{R}})}{\eta_{\mathrm{HPP}}} \tag{9}$$

where η_{MMP}, η_{hpp} and η_{PX} are the overall efficiencies of the mid- and high-pressure feed pumps and pressure exchanger, respectively; Q_{R} is the flow rate of the retentate,

$Q_R = Q_F - Q_P$; P_1^R , P_2^R and P_2^F are the outlet pressures of the first- and second-stage RO, and the inlet pressure of the second-stage RO, respectively.

The total work requirement of the IWRO treatment process is modeled by:

$$E_W = W_{IP} + W_{MMP} + W_{HPP} \tag{10}$$

Besides, considering the variability of environmental conditions, external hot and cold utilities are embedded in this model to determine the desired temperature of feed stream especially in extreme ambient temperature. The heat/cold utilities consumption is estimated by the following equation.

$$E_{HX} = Q_F \left| \left(T_F - T_A \right) \right| CP_F \tag{11}$$

where T_A is the ambient temperature and CP_F is the volume heat capacity of the feed stream.

3.3 Economics model

The economics model includes both operating and capital expenses of the system. The direct capital costs are mainly composed of the intake pumping and pretreatment (CC_{IPP}), the mid- and high-pressure feed pumps (CC_{MMP} and CC_{HPP}), the membrane elements (CC_{MEM}), and the pressure exchangers (CC_{PX}) for the initial installation as given by Eqs. 12~16. The total direct cost is given by Eq. 17.

$$CC_{IPP} = C_{IPP} (Q_F)^{n_1} N_{IPP} \tag{12}$$

$$CC_{MMP} = C_{MMP} \left[Q_F (1 - Sp) \Delta P_{MMP} \right] N_{MMP} \tag{13}$$

$$CC_{HPP} = C_{HPP} \left[Q_F (1 - RR_1) \Delta P_{HPP} \right] N_{HPP} \tag{14}$$

$$CC_{MEM} = C_{MEM} \sum_{i=1,2} N_i^e N_i^{pv} \tag{15}$$

$$CC_{\mathrm{PX}} = C_{\mathrm{PX}}\left[Q_{\mathrm{F}}(1-RR_1)(1-RR_2)\right]^{n_2} \tag{16}$$

$$CC_{\mathrm{DC}} = CC_{\mathrm{IPP}} + CC_{\mathrm{MMP}} + CC_{\mathrm{HPP}} + CC_{\mathrm{MEM}} + CC_{\mathrm{PX}} \tag{17}$$

where C and N denote the investment benchmark and the number of equipment. The subscripts IPP, MMP, HPP, MEM, and PX stand for the corresponding equipment, respectively. Note that the pumps approximately have a 10-year lifespan. In order to ensure there are enough pumps for the 25-year lifetime of the plant, in Eqs. 12-14 we assume that four of each pumping system (IPP, MMP, HPP) are purchased and three to be used within the lifetime of the plant and one as a backup. (Williams et al., 2012)

In order to reflect the additional capital investment (e.g., site development, land, and contracting), a practical investment factor (PIF) is used to evaluate the total capital cost by multiplying the total direct capital investment. In addition, the total capital cost is annualized by assuming that an annual interest rate (r) is paid over the plant lifespan (PL). Therefore, the annualized total capital cost is given by:

$$CC_{\mathrm{TOT}} = \mathrm{PIF} \times CC_{\mathrm{DC}} \times \frac{r \times (r+1)^{\mathrm{PL}}}{(r+1)^{\mathrm{PL}} - 1} \tag{18}$$

The operating cost includes mainly the chemical dose for pretreatment (OC_{chem}), the membrane cleaning and replacement for the membrane elements (OC_{MEM}), the energy cost for run the pump equipment and heat exchangers (OC_{energy}), and the cost for pressure exchange (OC_{PX}), as given by Eqs. 19~22, respectively. The total annual operating cost based on an operation time (OT) of 8000 hours per year is given by Eq. 23.

$$OC_{chem} = p_{chem} Q_{\mathrm{P}} \tag{19}$$

$$OC_{\mathrm{MEM}} = 2OC_{fixed} + \sum_{i=1,2} (0.25OC_{clean}S_i^E + 0.1CC_{MEM})N_i^e N_i^{pv} \tag{20}$$

$$OC_{energy} = p_{elec} \times E_{\mathrm{W}} + p_{uti} \times E_{\mathrm{HX}} \tag{21}$$

$$OC_{\mathrm{PX}} = 0.02CC_{\mathrm{PX}} \tag{22}$$

$$OC_{\mathrm{TOT}} = (OC_{pump} + OC_{chem} + OC_{\mathrm{PX}} + OC_{\mathrm{MEM}})OT \tag{23}$$

where O_{chem} stands for the annual chemical cost for unit permeate produced; p_{elec} and p_{uti} stand for the purchase prices for electricity and utility, respectively. In Eq. 20, it assumed that a fixed cost (OC_{fixed}) to replace or clean membranes along with a specific cost of per m^2 cleaned (OC_{clean}). It is also assumed that 25% of all membranes are cleaned annually while 10% are replaced.

The final economic equation for the total annualized cost (TAC) includes the operating cost and annualized capital cost, as given by

$$TAC = CC_{\mathrm{TOT}} + OC_{\mathrm{TOT}} \tag{24}$$

3.4 Multi-scenario model

As above-mentioned, great uncertainties related to saline wastewater data from coal-chemical EIPs could strongly hamper the process design and operation tasks of the IWRO treatment system. The traditional deterministic approach ignoring parametric variability would lead to a weak or idealized performance of the system represented by sub-optimal solutions. In this work, we develop a multi-scenario stochastic model by modifying the deterministic formulation to fully account for the diverse nature of wastewater variability in the IWRO treatment system, which is based on the correlated scenarios generation approach proposed by (Onishi et al.,

2017a; Onishi et al., 2017b). In this stochastic model the uncertain design parameters are mathematically modelled as a finite set of correlated feeding scenarios with known probability of occurrence.

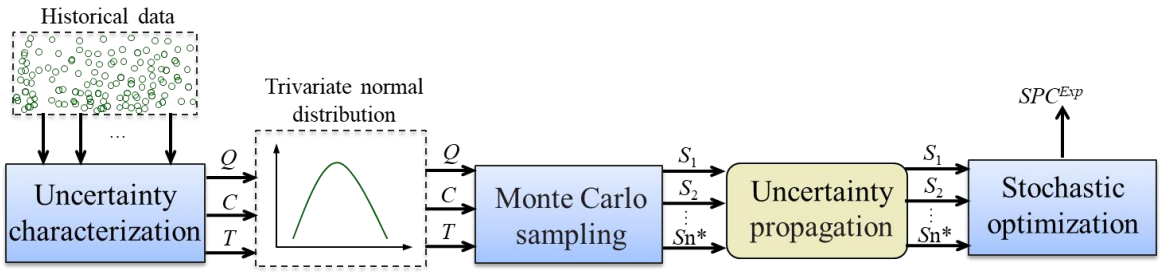

Figure 2. Illustration of the calculation procedure

In particular, as shown in Fig.2, this stochastic approach generally includes the following three steps as follows. (Shastri and Diwekar, 2010; Subramanyan et al., 2011) ***Step I***: characterization and quantification of uncertainty in terms of multivariate probability distributions. The amount of information available for the uncertain parameters of interest determines which type of distribution can be used in the uncertainty characterization. For instance, a Gaussian distribution can reflect a symmetric but varying probability of a parameter value being below or above the expected value. (Subramanyan et al., 2011) ***Step II***: data sampling from these multivariate distributions. A proper number of scenarios and the corresponding random values restricted by the distribution boundaries are generated via an efficient data sampling technique (e.g., Monte Carlo sampling and Latin hypercube sampling). S***tep III***: propagating the effects of uncertainty through performing a detailed techno-economic modeling including mass and energy balances, economic equations, and global constraints for each feeding scenario, as has been described in sections 3.2 and 3.3.

In Step II, it should be noted that a generated scenario corresponds to a single sample point of the multivariate probability distribution. In practice, the uncertain parameters normally have a symmetric relationship that affects the final distribution of sampling points in the space of interest. (Onishi et al., 2017b) For example, it is well-known that the in EIPs the salinity profile of a feed wastewater stream shows an evident growth as its flowrate drops especially in the cold season. Assuming that the uncertain parameters are subject to multivariate Gaussian distributions, the correlated scenarios can be generated using a pseudorandom number generator in MATLAB toolbox (*i.e.*, *mvnrnd* function). The probability density function for correlated random variables $\boldsymbol{X}_1,\ldots,\boldsymbol{X}_d$ with sample size n is given by:

$$f_{\mathrm{X}}(x)=\frac{1}{\sqrt{(2\pi)^n\det(\Sigma)}}\exp\left[-\frac{1}{2}(X-\mu)^T\Sigma^{-1}(X-\mu)\right] \tag{25}$$

where μ_i and det(Σ) are the mean value of each random variable and the determinant of covariance matrix $d\boldsymbol{X}d$. The diagonal elements of Σ containing the variances for each variable (σ_i^2) form a symmetric positive definite matrix. The off-diagonal elements that describe the implying correlation between the uncertain parameters, as given by

$$\sigma_{ij}=\rho_{ij}\sqrt{D(X_i)}\sqrt{D(X_j)}=\rho_{ij}\sigma_i\,\sigma_j \tag{26}$$

where ρ_{ij} and σ_{ij} denote the correlation matrix and covariances between variables, respectively. Note that ρ_{ij} contains the information on each pair of correlated variables by setting all non-diagonal elements with a value between -1 and 1. (Onishi et al., 2017a) Herein, a value ranging between -1 and 0 indicates a negative correlation, while 0~1 indicates a positive correlation. In addition, ±1 mean the strongest

correlation and 0 means non-correlation. That is, as ρ_{ij} =0 the covariance matrix would become a diagonal matrix that means the uncertain variables are independent and uncorrelated.

The model accuracy generally can be improved when more scenarios/samples are taken into account during the stochastic modeling and optimization. However, the computational burden will increase accordingly to obtain an optimal solution of the mean value of an objective function distribution. (Law et al., 1991; Onishi et al., 2017b). This entails a need to find a trade-off between accuracy and computational burden that determines the minimum size of scenarios used in the stochastic model. The desired level of accuracy of the solution can be measured by the confidence interval of the mean value of uncertain parameter with sample size n. In this work, a sampling variance estimator is used to estimate the confidence interval:

$$\mathrm{var}(n) = \sqrt{\frac{\Sigma_{s=1}^{n}[E(X^{(*)} - X^{(s)})]^2}{n-1}} \tag{27}$$

where $n=n_0+\Delta n$; $X^{(*)}$ and $X^{(s)}$ are the mean values of an uncertain parameter and the sampled value that corresponds to scenario s. Based on this sampling variance estimator, we can obtain the confidence level of 1-α, as given by

$$P\left[E(X^{(*)}) - \frac{z_{\alpha/2}\cdot var(n)}{\sqrt{n}},\ \ E(X^{(*)}) + \frac{z_{\alpha/2}\cdot var(n)}{\sqrt{n}}\right] \geq 1-\alpha \tag{28}$$

in which $z_{\alpha/2}$ is the standard normal deviation, $z \sim \mathbf{N}(0, 1)$ and $P(z \leq z_{\alpha/2})=1-\alpha/2$. For instance, for 98% confidence interval (1-α=98%), we have $z_{\alpha/2}$=2.06. Given the $var(n)$ and the confidence interval δ, the minimum size of scenarios can be obtained by Eq. 29. In this equation, we can resample from the multivariate distribution by updating

the sample size ($n=n_0+\Delta n$) until the desired confidence interval is reached ($\delta \leq \delta_d$). The final sample size (n^*) is regarded as a good approximation of the original distribution.

$$n^* = \left[\frac{z_{\alpha/2} var(n)}{\delta} \right]^2 \tag{29}$$

3.5 Stochastic objective function

The original problem involved in this work is a deterministic model where a single set of process variables are considered to obtain the specific production cost (SPC, denotes desalination cost per m^3 of permeate product) for the IWRO desalination system, as given by Eq. 30. As such, this deterministic approach only accounts for representative data of inlet saline water (flowrate, salinity, and temperature) in a single scenario.

$$\begin{aligned} &\text{(P1)} \quad \min \quad SPC = TAC / Q_{\mathrm{P}} \\ &\qquad \text{s.t.} \quad \text{Eq.(1)} \sim \text{Eq.(24)} \end{aligned} \tag{30}$$

The multiple scenarios generated in section 3.4 together with their corresponding probabilities can be used as input data for optimizing the stochastic optimization model. Unlike the deterministic approach, this stochastic approach can provide the major system flexibility under variability of uncertain parameters. In this work, the stochastic model is optimized to obtain robust solutions by minimizing the mean value of the objective distribution for the IWRO desalination system, as shown in the following equation.

$$\begin{aligned} &\text{(P2)} \quad \min \quad SPC^{Exp} = \sum_{s=1}^{n^*} prob_s SPC_s = \sum_{s=1}^{n^*} prob_s (TAC / Q_{\mathrm{P}})_s \\ &\qquad \text{s.t.} \quad \text{Eq.(1)} \sim \text{Eq.(24)} \end{aligned} \tag{31}$$

where $prob_s$ denotes the probability of occurrence of a specific feeding scenario s, note that this stochastic model assumes the same probability for all scenarios; SPC_s denotes the desalination cost for the same scenario, $SPCs = (TAC/Q_P)_s$. Note that in this stochastic model the equipment capacities (such as membrane elements and pressure vessels) should be the same for all scenarios and thus the capital cost belongs to the scenario-independent variable, while the operating expenses are formulated by stochastic functions to capture all variability in the uncertain search space. Overall, the optimization problem is a multi-scenario mixed-integer nonlinear program (MINLP) model. In each MINLP model, it consists of a single integer variable stated in Eq. 3 and multiple non-linear and linear variables.

4. Illustrative example

The developed model is illustrated next with a case study from a real-world EIP located in Shaanxi province, China. All coal-chemical plants located in this industrial park share a centralized saline wastewater desalination facility. In the present study, the single scenario considered in the deterministic model corresponds to the expected values for the basic plant data (e.g., 4000 $mg \cdot L^{-1}$ for the wastewater salinity and 500 $m^3 \cdot hr^{-1}$ for the flowrate). To simplify the optimization model, in the stochastic model we only consider two representative seasons (summer and winter) and three uncertain parameters related with the feed stream (volumetric flow rate, salinity, and inlet temperature) for the saline wastewater treatment system. Furthermore, it is assumed that the flowrate and salinity of feed wastewater are negatively correlated, while the flow rate and temperature have a positive correlation. This assumption is made due to

the fact that the salinity profile of the wastewater usually shows an increasing trend as the flow rate (temperature) is reduced especially in the summer.

For the sake of improving the robustness of the model, we also assume that the standard deviations of 5%, 10%, and 20% from the design flow rate and salinity due to the lack of detailed statistics for the inlet saline wastewater. The statistics of daily average dry bulb temperature during 2015-2017 retrieved from the National Oceanic and Atmospheric Administration (NOAA) database is used to construct the seasonal probability distribution function and the corresponding statistical distribution parameters. In this case, for each season the uncertainty on feed data is mathematically modeled using 100 distinct scenarios, which are the minimum number of scenarios generated by the proposed sampling technique with 95% confidence interval. Therefore, a total number of 200 scenarios are taken into account in the deterministic model, which can be considered as a good approximation of the original distribution throughout a year. More details of these scenarios can be found in an Excel file named Sample in Supporting Information. After that, the multi-scenario MINLP models are implemented using GAMS 24.4 modeling environment with global solver ANTIGONE (Misener and Floudas, 2014) and solved on a workstation with an Intel Core i7 at 3.8 GHz with 32 GB memory. In order to guarantee a global solution, we employ the following three simplification strategies: (1) auxiliary big-M variables and constraints to linearize the bilinear terms; (2) approximation of the concave terms by piecewise linear functions; (3) appropriate bounds and initial values

for all variables, as well as a bigger optimality gap such as 10^{-3}. The final reports show that the optimal solutions for all cases can be obtained within 20~120 min.

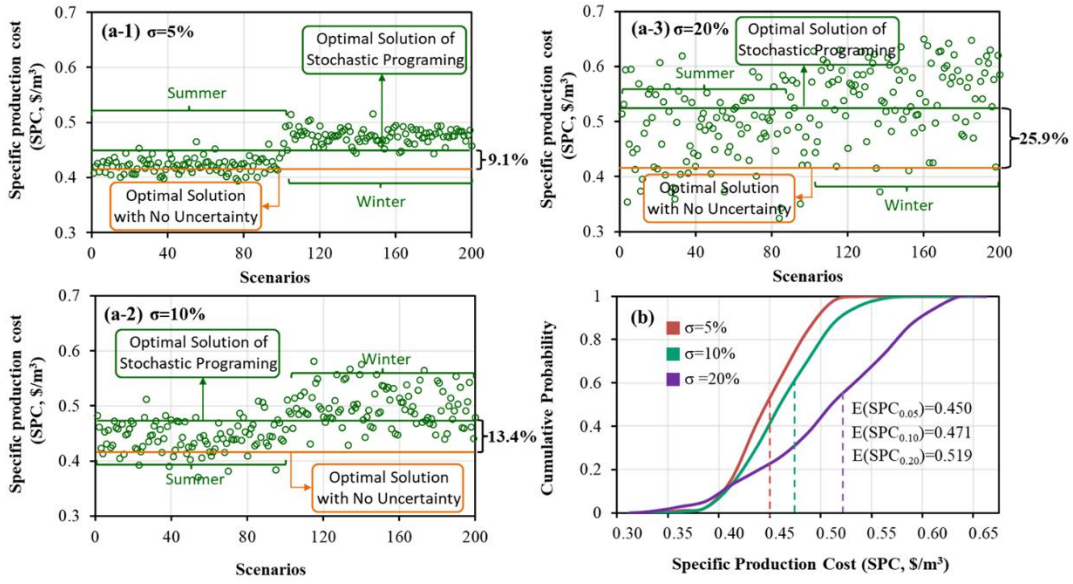

Figure 3. Specific production cost distribution obtained via stochastic and deterministic approaches and the cumulative probability distribution. (a-1~a-3) σ=5%, 10%, and 20%; (b) cumulative probability distribution.

In Fig. 3a presents the optimal solutions obtained by means of the stochastic and deterministic approaches for evaluating the impact of uncertainties on system performance regarding specific production cost. For better understanding the impact of uncertainty, the values of the green circles indicated in Fig. 3a are rearranged according to their corresponding cumulative probability distributions, as shown in Fig. 3b. As depicted, the yellow line in Fig. 3a is the exact objective value based on perfect information (no uncertainty) on feed data by solving the deterministic model, which is a fixed value $\$0.413 \cdot m^{-3}$. The green hollow circles are the objective values based on uncertainty on feed data from the stochastic model. The green line show the average performance of the stochastic model in terms of the mean value of specific

production cost, which is $E(SPC_{0.05})$=\$0.45·m^{-3} as σ=5%, $E(SPC_{0.10})$=\$0.471·m^{-3} as σ=10%, and $E(SPC_{0.20})$=\$0.519m^{-3} as σ=20%. The mean values of specific production costs obtained from stochastic model are 9.1%, 13.4%, and 25.9% higher than that of the deterministic model. This widening gap between the yellow line and green line implies that the deviation of feed data can remarkably pose great impacts on the system performance of the desalination system. Besides, by comparing the results of former 100 scenarios (summer) and later 100 ones (winter), it is noted that the specific production cost in cold season is relatively higher than that in hot season, while this tendency will be unapparent as σ increases from 5%, 10% to 20%. This phenomenon reflects that the increase in salinity of the wastewater in winter would contribute more portion to the production cost, compared with the increase in flowrate in summer.

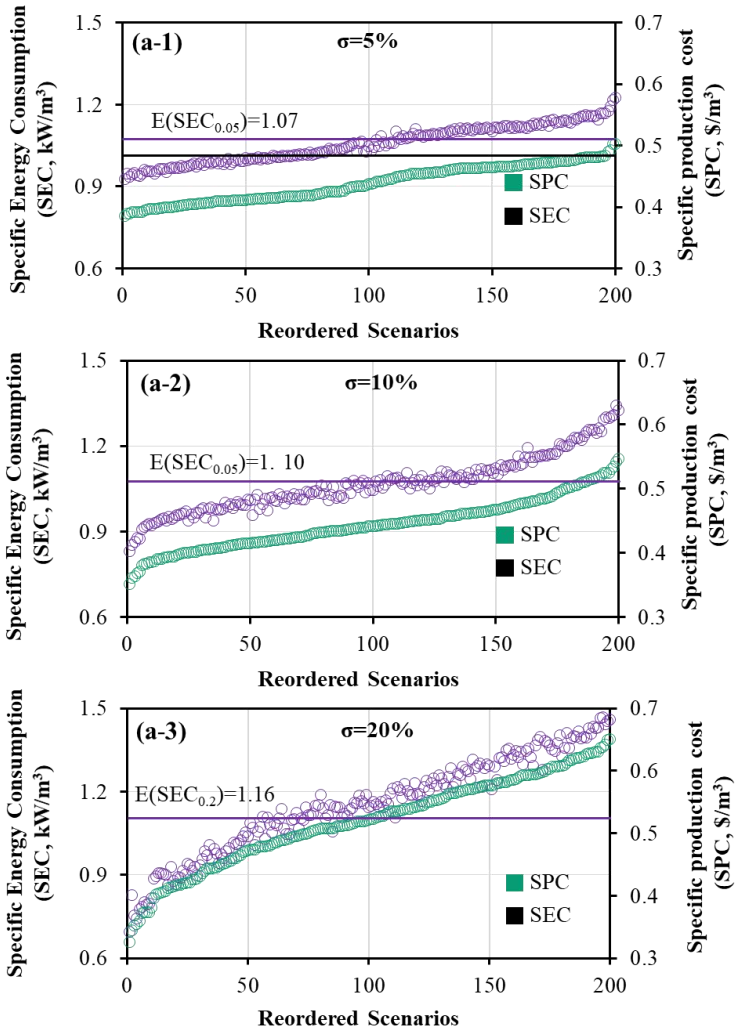

Figure 4. Distributions of specific energy consumption and production cost obtained via stochastic approach (a-1) σ=5%; (a-2) 10%; (a-3) σ=20%

Fig. 4 presents the specific energy consumption and production cost throughout the different feeding scenarios. For convenience, it is noted that in this figure all scenarios are resorted by ascending order of specific production cost. It is can be seen that the profile of specific energy consumption in general has a similar increasing trend with that of the specific production cost. In this figure, as the standard deviation of feed data increasing from 5% to 20%, the variation of production cost become more apparent throughout the different feeding scenarios. For instance, as σ=5%, SEC has a 32% increase from 0.93 $kW \cdot m^{-3}$ to 1.23 $kW \cdot m^{-3}$, while as σ=20%, SEC sharply

increases by 112% from 0.49 $kW \cdot m^{-3}$ to 1.46 $kW \cdot m^{-3}$. However, it is interesting that the mean value of energy consumption is relatively insensitive to the increase in standard deviation of feed data, i.e., as σ has a fourfold growth from 5% to 20%, E(SEC) only grows by 8.4% from 1.07 $kW \cdot m^{-3}$ to 1.16 $kW \cdot m^{-3}$. Meanwhile, E(SPC) has a greater growth by 15.3% from \$0.45$\cdot m^{-3}$ to \$0.519$\cdot m^{-3}$.

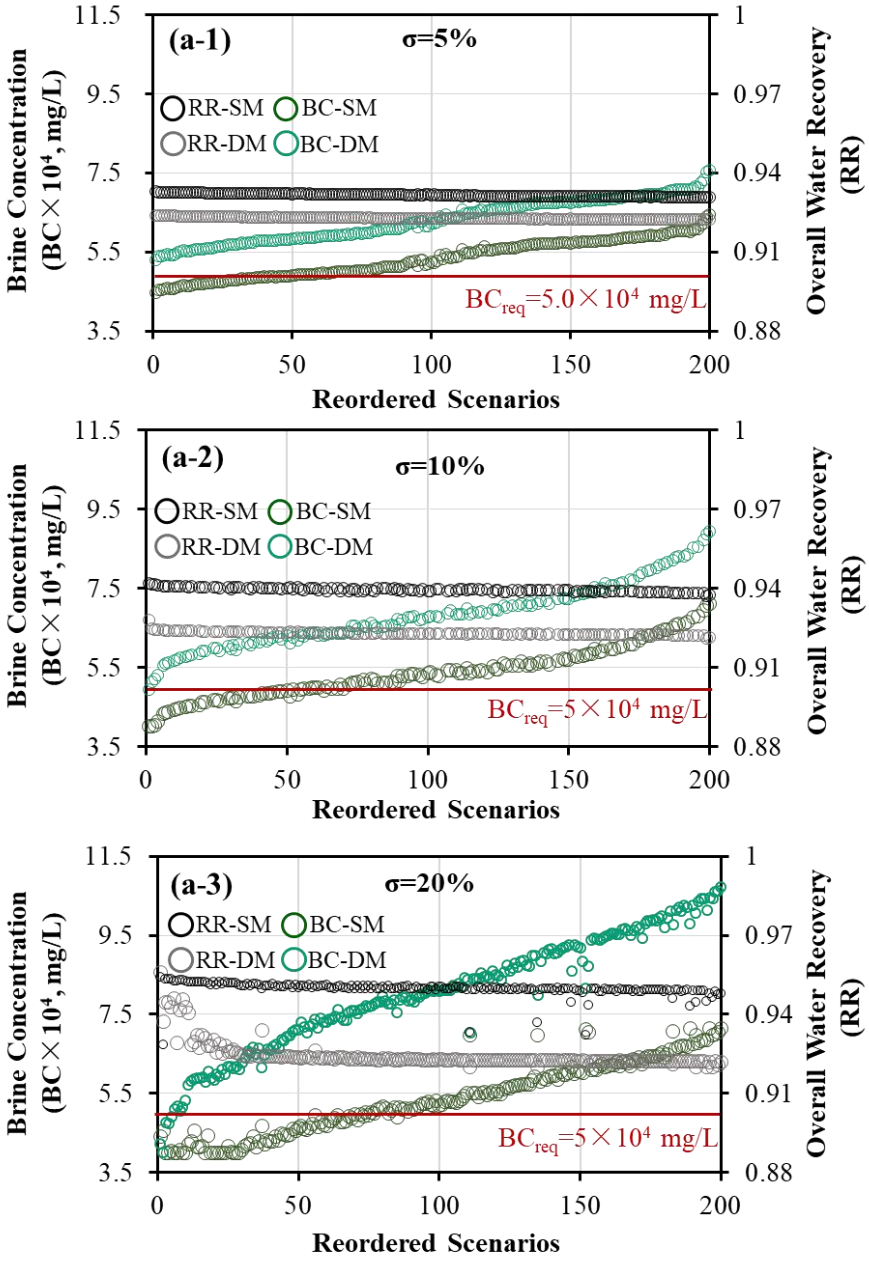

Figure 5. Distributions of brine concentration (BC) and overall water recovery (RR) throughout the different feeding scenarios obtained by solving stochastic model (SM) and deterministic model (DM). (a-1) σ=5%; (a-2) 10%; (a-3) σ=20%.

In general, the IWRO desalination system should be operated at a relatively high-level of overall water recovery to meet the concentration requirement for the outlet brine rejected from the second stage RO. This is due to high-salinity of outlet brine is beneficial for the operation of downstream posttreatment processes like mechanical vapor recompression and salt crystallization. According to the advice and industrial experience of plant engineers, it is considered that the minimum requirement for outlet brine concentration (BC_{req}) is 50,000 mg·L. In Fig. 5, we present the distribution profiles of both brine concentration and overall water recovery throughout the various feeding scenarios determined by the deterministic and stochastic approaches. Note that in this figure, the uncertainty on feed data is also considered in the deterministic model where the plant capacity is fixed and the feed data is varied depending on the feeding scenarios. As shown, for all cases the overall water recoveries are higher than 90%, especially for the results obtained via stochastic approach (RR=93%~95%). For the stochastic model, the increase in standard deviation of feed data leads to the water recovery to slightly improve by 2%~4%. In addition, the gap between the stochastic model and deterministic model becomes widener with the increasing σ. i.e., in Fig. 5(a-3), the mean value of water recovery is 95.0% for the stochastic model and is 92.4% for the deterministic model. Note that, a higher water recovery helps to decrease the salty concentration of the outlet brine. As such, it can be found that for the stochastic approach only 5 feeding scenarios shown

in the lower left quarter of Fig. 5(a-3) are not satisfying the concentration requirement for the outlet brine, while for the deterministic approach the unsatisfactory feeding scenarios sharply increase to 36, 52, and 73 as σ=5%, 10%, and 20%, respectively. Form the comparison, we conclude that the optimal solution obtained via deterministic model based on the mean values of plant data in the whole year can incur significant variance of system performances depending on the exact realization of uncertainty.

The mean values of total annualized cost obtained via stochastic approach are provided in Fig. 6, where the cost can be divided into operating cost and capital investment. As shown, the total annualized cost increases from $1.93MM as σ=5%, to $2.09MM as σ=5%, and to $2.41MM as σ=20%. For each standard deviation, the capital investment contributes 62.1%~65.3% of the total cost and the remaining contribution comes from the operating cost. It is interesting that though the operating cost has a slight growth from σ=5% to σ=20%, the corresponding proportion declines from 37.9% to 34.6%. This phenomenon can be attributed to the fact that the operating cost takes a smaller proportion and is less sensitive to the increase in the deviation of feed data.

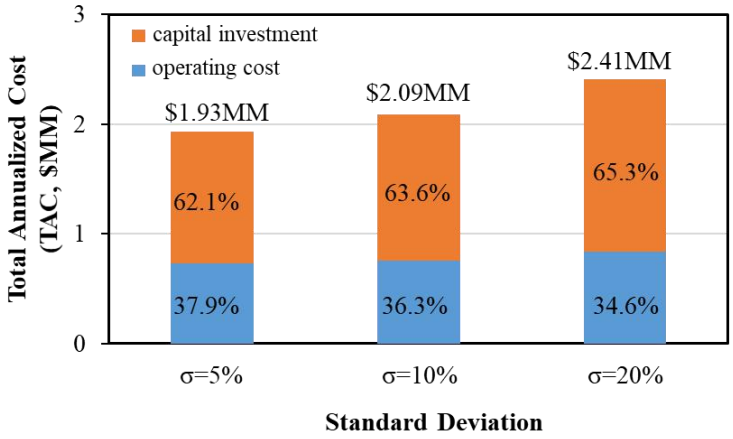

Figure 6. The mean values of total annualized cost under different standard deviations

Fig. 7 further presents the detailed cost breakdowns of the total annualized cost that corresponds to σ=20% shown in Fig.6. From right hand of this cost breakdown, it is clear that the electricity and membrane replacement account for the major operating costs. The remaining contributions come from pretreatment, heat utility, and pressure exchanger. Note that, this work considers that all uncertain parameters are subject to multivariate normal distribution and are varied around their mean values. The operating cost is mostly defined by the stochastic function (see Eq.31) to capture all variabilities of the electricity consumption and membrane replacement in the uncertain space. This indirectly makes the optimal solution of operating costs obtained via stochastic model would constantly increase or decline depending on the realization of uncertainty. Contrarily, in the stochastic model the capital cost belongs to the scenario-independent variable. The stochastic approach inclines to overdesign the IWRO system to reduce the occurrence probability of unsatisfactory system performances (i.e., low water recovery and outlet brine concentration) under extreme scenarios. Meanwhile, the economic costs behind the improved robustness under feed

data uncertainty is also noticeable. For example, as standard deviation increases from 5% to 20%, the quantity of pressure vessels installed in the first-stage RO has a remarkable increase from 49 to 73. As shown in Fig. 7, the capital investment has increased by \$0.37MM from \$1.2 MM to \$1.57 MM. One possible way to reduce economic risk as the capital investment is higher than the operating expense since that a process design with minimum expected operating expense normally possess minimum risk.

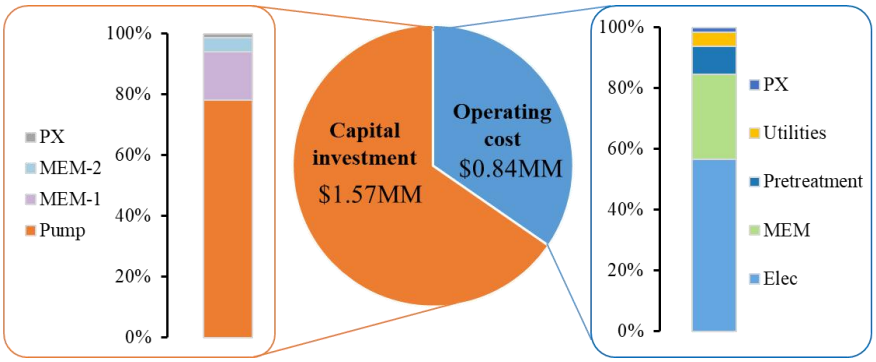

Figure 7. Breakdown of total annualized cost (σ=20%)

5. Conclusions

It is of significant importance to consider the uncertainty on feed data when design an industrial wastewater desalination process. This work has addressed the optimal design of a duel-stage IWRO desalination under uncertainty by proposing a multi-scenario MINLP optimization model. In order to properly describe the wastewater variability, multiple uncertain design parameters including salt concentration, flowrate, and inlet temperature of feed wastewater were all taken into account for the exact realization of uncertainty. Furthermore, a three-step stochastic data processing strategy including uncertainty characterization and quantification,

data sampling, data propagation has developed to generate a finite size of correlated feeding scenarios. The detailed model of the dual-stage RO was incorporated in the objective function in order to minimize the specific production cost.

An illustrative example from a coal-chemical EIP was used to evaluate the applicability of the proposed model. The results indicated that the expected specific production costs obtained from stochastic model are 9.1%, 13.4%, and 25.9% higher than that of the deterministic model as the standard deviations varies from 5%, 10%, and 20%, respectively. However, these economic costs brought significant benefits for the system's robustness and reduced risks in performances under uncertainty. It was found that for the stochastic approach only 5 feeding scenarios in total are not satisfying the quality requirement for the outlet brine, while for the deterministic approach the unsatisfactory feeding scenarios sharply increase to 36, 52, and 73 as σ=5%, 10%, and 20%, respectively.

Acknowledgement

Financial supports from the National Natural Science Foundation of China (No. 21606261, 51776228) and the Major Projects for Science and Technology of Gansu Province (No.18ZD2GD014) are gratefully acknowledged.

Reference

Abass, M., Majozi, T., 2016. Optimization of integrated water and multiregenerator membrane systems. Industrial & Engineering Chemistry Research 55(7), 1995-2007.

Andiappan, V., Tan, R.R., Ng, D.K.S., 2016. An optimization-based negotiation framework for energy systems in an eco-industrial park. Journal of Cleaner Production 129, 496-507.

Asatekin, A., Kang, S., Elimelech, M., Mayes, A.M., 2007. Anti-fouling ultrafiltration membranes containing polyacrylonitrile-graft-poly (ethylene oxide) comb copolymer additives. Journal of Membrane Science 298(1-2), 136-146.

Da A., Xi B., Ren J., Wang Y., Jia X., Chang H., Li Z., 2017. Sustainability assessment of groundwater remediation technologies based on multi-criteria decision making method, Resources, Conservation and Recycling 119, 36-46.

El-Halwagi, M.M., 1997. Pollution prevention through process integration: systematic design tools. Elsevier.

FILMTEC™, D., 2018. FLMTECTM Reverse Osmosis Membranes Technical Manual.

Gençer, E., Agrawal R., 2018. Toward supplying food, energy, and water demand: Integrated solar desalination process synthesis with power and hydrogen coproduction, Resources, Conservation and Recycling 133, 331-342.

Ghobeity, A., Mitsos, A., 2010. Optimal time-dependent operation of seawater reverse osmosis. Desalination 263(1-3), 76-88.

Gupta, V.K., Ali, I., Saleh, T.A., Nayak, A., Agarwal, S., 2012. Chemical treatment technologies for waste-water recycling—an overview. Rsc Advances 2(16), 6380-6388.

Karuppiah, R., Bury, S.J., Vazquez, A., Poppe, G., 2012. Optimal design of reverse osmosis-based water treatment systems. AIChE Journal 58(9), 2758-2769.

Khor, C.S., Chachuat, B., Shah, N., 2012. A superstructure optimization approach for water network synthesis with membrane separation-based regenerators. Computers & Chemical Engineering 42, 48-63.

Law, A.M., Kelton, W.D., Kelton, W.D., 1991. Simulation modeling and analysis. McGraw-Hill New York.

Li, M., 2015. Analysis and optimization of pressure retarded osmosis for power generation. AIChE Journal 4, 1233.

Lu, Y.-Y., Hu, Y.-D., Zhang, X.-L., Wu, L.-Y., Liu, Q.-Z., 2007. Optimum design of reverse osmosis system under different feed concentration and product specification. Journal of membrane science 287(2), 219-229.

Malaeb, L., Ayoub, G.M., 2011. Reverse osmosis technology for water treatment: state of the art review. Desalination 267(1), 1-8.

Misener, R., Floudas, C.A., 2014. ANTIGONE: Algorithms for coNTinuous / Integer Global Optimization of Nonlinear Equations. Journal of Global Optimization 59(2), 503-526.

Onishi, V.C., Ruiz-Femenia, R., Salcedo-Díaz, R., Carrero-Parreño, A., Reyes-Labarta, J.A., Fraga, E.S., Caballero, J.A., 2017a. Process optimization for zero-liquid discharge desalination of shale gas flowback water under uncertainty. Journal of Cleaner Production 164, 1219-1238.

Onishi, V.C., Ruiz-Femenia, R., Salcedo-Díaz, R., Carrero-Parreño, A., Reyes-Labarta, J.A., Caballero, J.A., 2017b. Optimal shale gas flowback water desalination under correlated data uncertainty, Computer aided chemical engineering 40, 943-948.

Park, C., Park, P.-K., Mane, P.P., Hyung, H., Gandhi, V., Kim, S.-H., Kim, J.-H., 2010. Stochastic cost estimation approach for full-scale reverse osmosis desalination plants. Journal of Membrane Science 364(1-2), 52-64.

Shastri, Y., Diwekar, U., 2010. Stochastic modeling for uncertainty analysis and multiobjective optimization of IGCC system with single-stage coal gasification. Industrial & Engineering Chemistry Research 50(9), 4879-4892.

Subramanyan, K., Diwekar, U., Zitney, S.E., 2011. Stochastic modeling and multi-objective optimization for the APECS system. Computers & Chemical Engineering 35(12), 2667-2679.

Tiu, B.T.C., Cruz, D.E., 2017. An MILP model for optimizing water exchanges in eco-industrial parks considering water quality. Resources, Conservation and Recycling 119, 89-96.

Wang, J., Dlamini, D.S., Mishra, A.K., Pendergast, M.T.M., Wong, M.C.Y., Mamba, B.B., Freger, V., Verliefde, A.R.D., Hoek, E.M.V., 2014. A critical review of transport through osmotic membranes. Journal of Membrane Science 454, 516-537.

Wang, S.H., Zhu, Q.P., He, C., Zhang, B.J., Chen, Q.L., Pan, M., 2018. Model-based optimization and comparative analysis of open-loop and closed-loop RO-PRO desalination systems, Desalination 446, 83-93.

Werber, J.R., Deshmukh, A., Elimelech, M., 2017. Can batch or semi-batch processes save energy in reverse-osmosis desalination? Desalination 402, 109-122.

Williams, C.M., Ghobeity, A., Pak, A.J., Mitsos, A., 2012. Simultaneous optimization of size and short-term operation for an RO plant. Desalination 301, 42-52.

Yang, L., Salcedo-Diaz, R., Grossmann, I.E., 2014. Water network optimization with wastewater regeneration models. Industrial & Engineering Chemistry Research 53(45), 17680-17695.

Zhu, Q., Zhang, B., Chen, Q., Pan, M., Ren, J., He, C., 2017. Optimal Synthesis of Water Networks for Addressing High-Concentration Wastewater in Coal-Based Chemical Plants. ACS Sustainable Chemistry & Engineering 5(11), 10792-10805.